Eur. Phys. J. AP **3**, 263–271 (1998)

THE EUROPEAN PHYSICAL JOURNAL APPLIED PHYSICS

Study methods of induction traction motor three phase short circuits

N. Retière[a] and M. Ivanès

Laboratoire d'Electrotechnique de Grenoble, INPG / UJF[b], E.N.S.I.E.G., rue de la Houille Blanche, B.P. 46, 38402 Saint-Martin-d'Hères Cedex, France

Received: 21 October 1997 / Revised: 16 June 1998 / Accepted: 16 June 1998

Abstract. The authors propose study methods of three phase short circuits of an induction traction motor. Methods are based on finite element model or equivalent circuits of the machine and take into account, more or less accurately, saturation and deep bar effects. Depending on the modeling level, they can be used to study short circuit torque or current maxima, waveforms or local constraints. The proposed methods are applied to a 1.5 MW - 4 pole traction motor short circuit study.

PACS. 84.50.+d Electric Motors – 84.37.+q Electric variable measurements – 07.05.Tp Computer Modeling and simulation

Nomenclature

p	number of poles pairs
Γ_{elm}	electromagnetic torque of the machine (Nm)
Γ_n	rated torque (Nm)
Γ_{max}	maximal amplitude of the short circuit torque (Nm)
$\boldsymbol{\varphi}_s$	stator flux space vector (Wb)
θ_s	angular position of $\boldsymbol{\varphi}_s$ in a stator reference frame (rad)
$\boldsymbol{\varphi}_r$	rotor flux space vector (Wb)
φ_s, φ_r	module of $\boldsymbol{\varphi}_s$ and $\boldsymbol{\varphi}_r$ (Wb)
γ	phase shift between $\boldsymbol{\varphi}_s$ and $\boldsymbol{\varphi}_r$ (rad)
i_a, i_b, i_c	machine phase currents (A)
i_{amax}	maximal value of (a) phase current (A)
$\mathbf{i}_s$	stator current space vector (A)
I_s	r ms value of $\mathbf{i}_s$ (A)
I_{sn}	rated rms value of $\mathbf{i}_s$ (A)
I_d	start-up current rms value (A)
I_{dn}	rated r ms value of start-up current (A)
$\mathbf{i}_r$	rotor current space vector (A)
$\mathbf{i}_m$	magnetizing current space vector (A)
$\mathbf{V}_s$	stator voltage space vector (V)
V_s	r ms value of $\mathbf{V}_s$ (V)
V_{sn}	rated r ms value of $\mathbf{V}_s$ (V)
Φ	initial angular position of $\mathbf{V}_s$ in a stator reference frame (rad)
$\boldsymbol{\varphi}$	phase shift between $\mathbf{i}_s$ and $\mathbf{V}_s$ (rad)
$\varphi_{\mathbf{n}}$	rated phase shift between $\mathbf{i}_s$ and $\mathbf{V}_s$ (rad)
$\varphi_{\mathbf{d}}$	start-up phase shift between $\mathbf{i}_s$ and $\mathbf{V}_s$ (rad)
ω_g	orthogonal winding s angular velocity in a stator reference frame (rad/s)
ω_s	stator voltage angular velocity in a stator reference frame (rad/s)
ω_{sn}	rated stator voltage angular velocity in a stator reference frame (rad/s)
f_s	stator voltage frequency (Hz)
Ω	rotor mechanical speed (rad/s)
ω	rotor angular velocity in a stator reference frame $= p\Omega$ (rad/s)
θ	rotor angular position in a stator reference frame (rad)
σ	leakage distribution factor
Z_s	operational impedance (Ω)
R_s	stator resistance (Ω)
R_r	stator referred resistance of rotor cage (Ω)
l_{σ^s}	stator leakage inductance (H)
l_{σ^r}	stator referred leakage inductance of rotor cage (H)
I_{σ^m}	stator referred mutual leakage inductance (H)
L_s	synchronous stator inductance (H)
L_r	rotor inductance (H)
L_m	magnetizing inductance (H)
τ_s, τ_r	stator and rotor open circuit time constant (s)
τ	average motor time constant (s)
T'	rotor transient time constant, stator in short circuit (s)
T_a	stator transient time constant, rotor in short circuit (s)
s	Laplace operator

[a] e-mail: Nicolas.Retiere@leg.ensieg.inpg.fr
[b] CNRS.UMR 5529

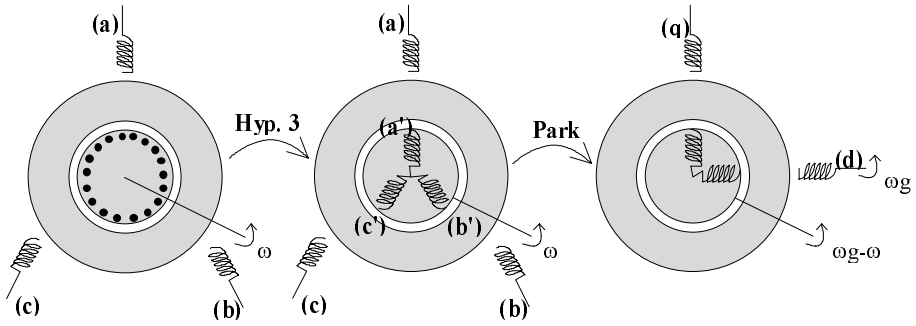

Fig. 1. Single cage induction machine modeling.

1 Introduction

Nowadays, voltage source induction motor drives are in current use for electric traction applications. Since converter failures yield to very large electromechanical transients [26], a systematic study of the faulty modes is required to increase reliability as to study monitoring, protection and post-recovery fault strategies [27,28].

This study could not be achieved without an acute analysis of machine behavior during large transient operations because the faulty operations may cause machine parameters variations and electromagnetic stresses.

Three phase short circuits are typical large transient operations of cage induction machines. They cause serious mechanical stresses because of the short circuit reverse torque peak [22]. Three phase short circuits study is all the more crucial as numerous large transient features can be so pointed out and discussed.

In this paper, three phase short circuits of a 1.5 MW - 4 pole traction motor are investigated and modeled. Depending on the purposes, several investigation and modeling methods can be proposed:

- Finite element method which enables local study of the short circuited machine and identification of equivalent circuits.
- Analytical formulation of the induction motor equations. Because of its extreme simplicity, this method is opposed to finite element formulation.
- Numerical solving of the motor equations. This method does not require the assumptions used for the analytical formulation and its application is far less complex than the finite element method one.

The chosen method might be able to provide some relevant information on short circuit current and torque.

2 Transient model of cage induction machine

2.1 Presentation

Transient electric equations of a cage induction machine are obtained under the following assumptions [1]:

- the core and mechanical losses are neglected;
- the machine is symmetric;
- both stator windings and rotor squirrel cage are replaced by 3-phase sinusoidally distributed windings. Hence, the effects of space harmonics are neglected.
- There is no saturation and other non-linearities.

In these conditions, an ideal machine can be derived from the real one (Fig. 1). This ideal machine is made from two orthogonal windings (d, q) rotating at ω_g in a stator reference frame. Depending on the use of the model, (d, q) windings are chosen fixed either to the stator ($\omega_g = 0$) or the rotor ($\omega_g = \omega$) or the rotating fields ($\omega_g = \omega_s$).

In a stator reference frame ($\omega_g = 0$), electric equations of the ideal machine can be expressed in a vector form by:

$$\begin{cases} \mathbf{V}_s &= R_s \mathbf{i}_s + \dfrac{d\boldsymbol{\varphi}_s}{dt} \\ \\ \mathbf{0} &= R_r \mathbf{i}_r + \dfrac{d\boldsymbol{\varphi}_r}{dt} - j\omega\boldsymbol{\varphi}_r. \end{cases} \tag{1}$$

Electromechanical conversion is expressed by the equation:

$$\Gamma_{elm} = pL_m \times Imag[\mathbf{i}_s \mathbf{i}_r^*]. \tag{2}$$

2.2 Equivalent circuit

The flux space vectors are expressed by:

$$\begin{cases} \boldsymbol{\varphi}_s &= L_s \mathbf{i}_s + L_m \mathbf{i}_r \\ \boldsymbol{\varphi}_r &= L_m \mathbf{i}_s + L_r \mathbf{i}_r \end{cases} \tag{3}$$

where :

$$\begin{cases} L_s &= L_m + l_{\sigma s} \\ L_r &= L_m + l_{\sigma r}. \end{cases} \tag{4}$$

Thus, equations system (1) can be represented by the equivalent circuit given in Figure 2 [2]. All the rotor parameters are referred to the stator.

To obtain this equivalent circuit, total leakage inductance is separated between stator and rotor parts. This separation is quite arbitrary. An other leakage flux partition can be supposed (for instance, it can be assumed $l_{\sigma^s} = 0$ or $l_{\sigma^r} = 0$) so that equivalent circuit parameters values are modified but terminal impedance and torque values are kept the same [3].

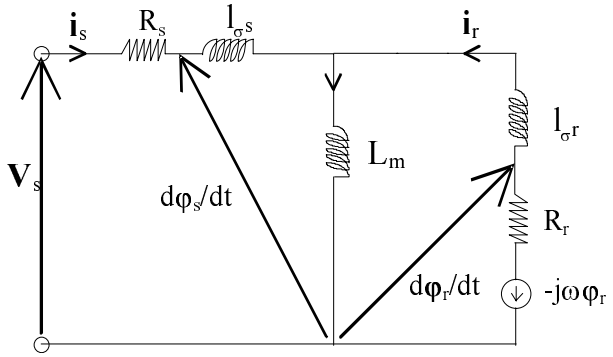

Fig. 2. Equivalent circuit of a single cage induction machine in a stator reference frame.

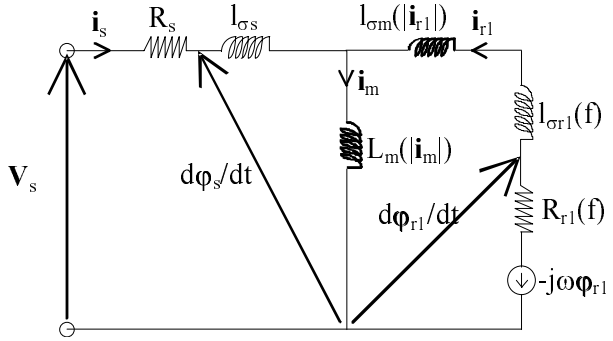

Fig. 3. Equivalent circuit of a saturated induction machine in a stator reference frame.

2.3 Consequences of the saturation

Saturated machines fed by sinusoidal sources have not a sinusoidal distribution of the air gap induction $B(\theta, t)$. But, if the winding distribution is sinusoidal, linkage flux $\Psi(t)$ is still sinusoidal since only fundamental component of $B(\theta, t)$ can produce it.

Variations of motor electric variables are thus still sinusoidal and the equivalent circuit can be defined if inductances are saturable which means they vary along with the current flowing through them [4–7].

Non linear inductance variations may be given by no load and blocked rotor tests performed by experience or finite element method [8].

In presence of saturation, leakage flux partition required for the equivalent circuit building is chosen so that only the rotor leakage inductance is saturable. But, owing to deep bar effect, rotor parameters can also vary along with the current frequency [2,9]. Thus, rotor leakage inductance is separated in two parts, modeling respectively the saturation and deep bar effects [4,7,10].

Finally, a cage induction machine operating in a saturated transient mode can be represented by the equivalent circuit as illustrated in Figure 3.

2.4 Validity of the equivalent circuit for the study of transient operations

Despite the assumptions, core losses can be approximately taken into account in the equivalent circuit by introducing additional resistances [5,6,11].

In the same way, space harmonic effects can be represented by adding leakage inductances [2]. At last, by solving together the equivalent circuit equations with the equation of motion, mechanical losses can be represented. Hence, only the assumptions of sinusoidal feeding and machine symmetry can not be get round by the proposed equivalent circuit. First assumption requires to consider an equivalent circuit for each source harmonic and second one yields to define an improved machine model based on finite element or matrix representations [1,6,12–14].

Hence, the solving of the differential equations of the model is usable to study numerous large symmetric transient operations and gives global results about waveforms and terminal impedance variations. However, it does not allow to understand motor internal behavior during the transient operations. An analysis method based on time stepping finite element computations is then preferred.

3 Study of three phase short circuits by the finite element method

3.1 Finite element modeling

Cage induction machine is modeled during transient operation by a bidimensionnal electromagnetic model which includes deep bar and saturation effects. The model is coupled with an electric circuit which enables to specify connections between voltage sources and stator winding s, to describe the rotor cage structure and to include end resistances and leakage inductances of machine windings [20].

Air gap is described by a mesh strip [21]. It allows to modify the rotor angular position at every time steps without meshing again stator and rotor areas.

The solution of Maxwell's equations is provided by a time stepping solving method [21] in two different reference frames: one fixed to the stator, the other moving with the rotor.

3.2 Finite element investigation

The model is used to compute three phase short circuits of a 1.5 MW - 4 poles cage induction motor designed for railway traction locomotives. In this case, it may reasonably be assumed that the mechanical speed remains constant during the short circuit operation.

A brief description of the finite element procedure is shown in Figure 4.

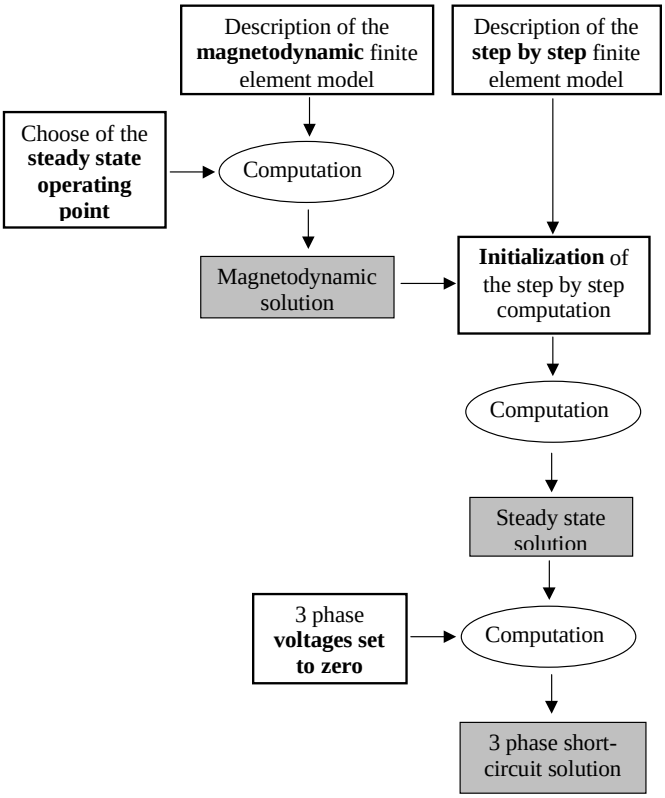

Fig. 4. Description of the finite element procedure.

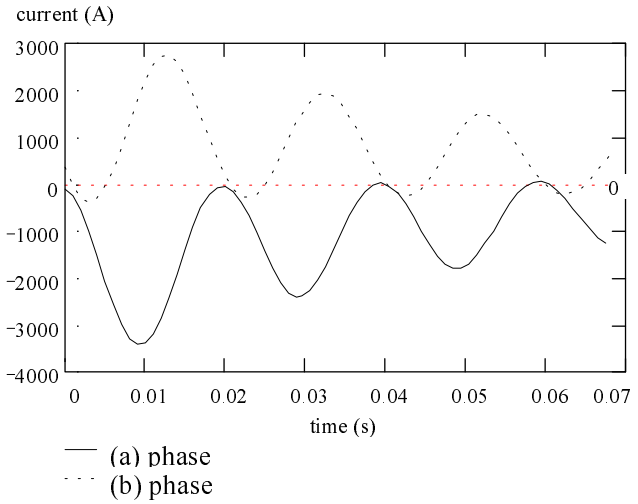

Fig. 5. Short circuit currents waveforms.

3.2.1 Numerical computation

The three phase short circuit is computed at a steady state operating point given by: $V_s = 1200$ V, $f_s = 51$ Hz, $\Gamma_{elm} = 11$ kNm, $\Omega = 29.3$ rad/s.

This steady state operation is obtained by a step by step finite element solving. In order to decrease the computation time, the solving is initialized from a finite element result given in complex magnetodynamic domain at the same operating point. The three phase short circuit is performed by setting to zero, at the same time, the three supply voltages. Then, phase currents and electromagnetic torque oscillate at a frequency near the initial supply frequency and are damped with time constants related with the stator winding s and rotor cage electric parameters [22] (Figs. 5 and 6).

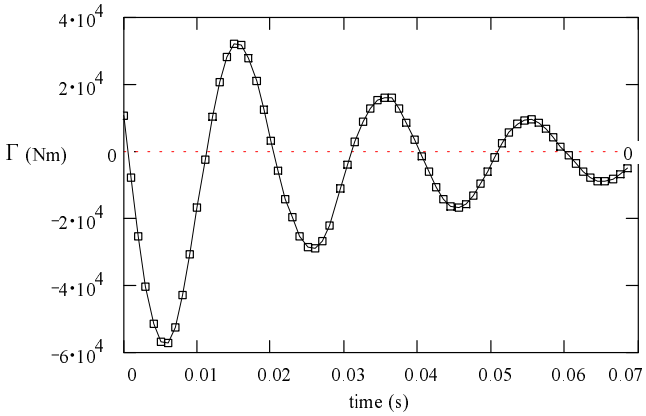

Fig. 6. Short circuit torque waveforms.

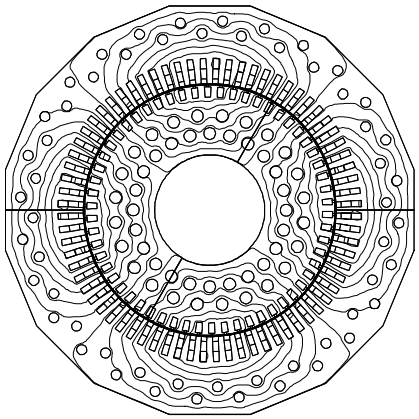

Fig. 7. Flux distribution at the initial time of the short circuit.

Finite element resolutions also provide the variations of the internal machine variables during the three phase short circuit.

3.2.2 Investigation of the electromagnetic state

Rotor slip is initially low and flux flow deeply in the rotor core (Fig. 7). Thus, the main flux path is highly saturated.

Because of the cancellation of the machine voltages, the short circuit yields to a quasi-fixed machine field. Indeed, in accordance with equation (1), the stator flux space vector variations are null if the resistive voltage drops are negligible.

The fixed field induces rotor cage currents oscillating at the rotation electric frequency of the rotor. Finally, the flux density wave created by the rotor winding s is a space wave rotating at the rotor electric pulsation. The consequences of this electromagnetic state on the flux path distribution are illustrated in Figures 7 and 8: stator flux path distribution remains near the same whereas rotor

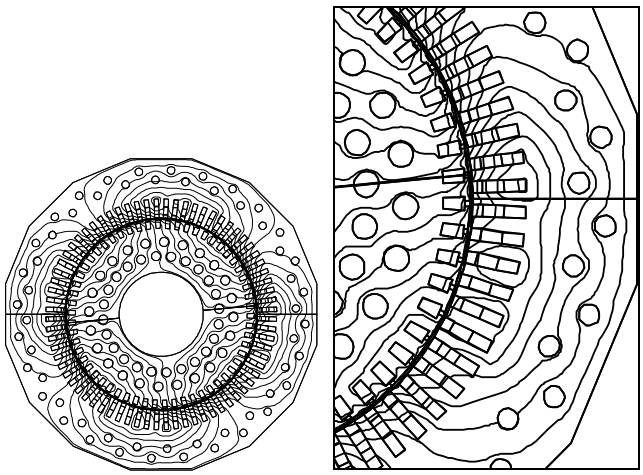

Fig. 8. Flux distribution at the maximum of short circuit torque.

one has rotated of about 1/8 round. These changes of the interaction between stator and rotor parts yield to torque oscillations as shown in Figure 6. Obviously, the maximal torque value is reached when stator and rotor flux are in quadrature (Fig. 8).

From the short circuit occurrence, there are only leakage flux. Hence, the main flux path is not anymore saturated while the rotor and stator teeth saturation level is high. This saturation level is increased by the large values of short circuit currents.

What is more, as rotor currents oscillate at near the rotor electric frequency, skin effect appears in the rotor bars.

As a result of these deep changes, a large transient model simpler than the finite element model should include the effects of local saturation, main flux path non saturation and current displacement at the operating frequency.

4 Analytical and differential approaches of three phase short circuits

Analytical approach enables easy understanding of complex phenomena and may provide relatively accurate results. The analytical approach introduced in this paper is based upon analytical formulation of the differential equations related with the classical single cage induction machine equivalent circuit as shown in Figure 2. These same equations can also be numerically solved. This is the differential approach.

4.1 Analytical approach

4.1.1 Principles

The issue of the method is to provide main features of torque and phase currents during the first instants of three phase short circuits. Calculations are extremely simplified by assuming that inductances are constant and damping effects are negligible. After analytical solving of the equations, effects of saturation and current displacement are included in the analytical formulation by modifying the parameters values.

Methodological assumptions are then:

- the machine operates in linear conditions;
- all the parameters of the equivalent circuit are constant and known;
- resistive voltage drops are neglected during the short circuit operation in comparison with reactive voltage ones;
- the stator resistance is neglected in the initial conditions expression;
- the rotor speed remains constant;
- the initial time of the short circuit is known.

According to the finite element simulation, three phase short circuits can be considered as the dual of induction machine start-up operations at the same operating point. Indeed, in both cases, stator and rotor behavior are decoupled. Moreover, start-up operations yield to simultaneous application of the supply voltages to the machine whereas three phase short circuits lead to their cancellation.

The purpose of the analytical formulation is therefore to link torque and phase current expressions with the initial conditions of the short circuit operation and the start-up current at the same operating conditions.

4.1.2 Analytical formulation of the differential equations

After Laplace transform and with respect to the methodological assumptions, the differential system (1) can be expressed by:

$$\begin{cases} L_s \mathbf{i}_s(s) + L_m \mathbf{i}_r(s) & = \dfrac{L_s \mathbf{i}_s^0 + L_m \mathbf{i}_r^0}{s} \\ L_r \mathbf{i}_r(s) + L_m \mathbf{i}_s(s) & = \dfrac{L_r \mathbf{i}_r^0 + L_m \mathbf{i}_s^0}{s - j\omega} \end{cases} \tag{5}$$

$\mathbf{i}_s(0) = \mathbf{i}_s^0$ et $\mathbf{i}_r(0) = \mathbf{i}_r^0$ are the initial conditions where $\mathbf{i}_s^0$ is given by:

$$\mathbf{i}_s^0 = I_s e^{-j\varphi}. \tag{6}$$

According to the simplified equivalent circuit ($R_s = 0$):

$$i_r^0 = -\frac{L_s}{L_m}\left(j\frac{V_s}{L_s\omega_s} + I_s e^{-j\varphi}\right). \tag{7}$$

The inclusion of (6) and (7) in (5) yields to the introduction of the variable I_d expressed by:

$$I_d = \frac{V_s}{\sigma L_s \omega_s} \tag{8}$$

I_d is the start-up current at the short circuit initial conditions (V_s, ω_s) when R_s and R_r are negligible.

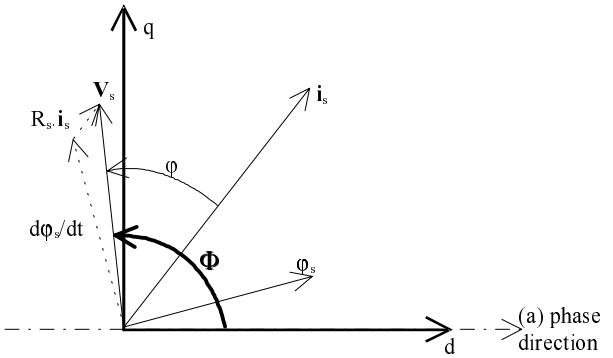

Fig. 9. Angular vector positions at the initial time of the short circuit.

After complete solving of (5) and inverse Laplace transform, (a) phase current expression is given by:

$$i_a(t) = I_d\sqrt{2}\,[\sin\Phi - \sin(\omega t + \Phi)] + I_s\sqrt{2}\cos(\omega t + \Phi - \varphi) \tag{9}$$

Φ is the short circuit initial angle as defined in Figure 9.

The short circuit electromagnetic torque can then be expressed by:

$$\Gamma_{elm}(t) = 3\frac{V_s I_s}{\frac{\omega_s}{p}}\cos(\omega t - \varphi) - 3\frac{V_s I_d}{\frac{\omega_s}{p}}\sin\omega t. \tag{10}$$

It should be noted that i_a and Γ_{elm} oscillate at the rotor electric pulsation ω.

4.1.3 Expression of torque and current maxima

Whatever the initial conditions are, start-up current I_d is always largely higher than steady-state current I_s. Hence, the maximal value of the short circuit torque can be given by the following approached expression:

$$\Gamma_{\max} = -3\frac{V_s I_d}{\frac{\omega_s}{p}}\,. \tag{11}$$

This value corresponds to the $\sin\omega t$ component amplitude obtained at the time t_m defined by: $\omega t_m = \pi/2$.

At constant V/f ratio, it can be shown that Γ_{max} is near independent of the initial conditions and is equal to the maximal value of the short circuit torque at nominal operating conditions. Then:

$$\Gamma_{max} = -\frac{I_{dn}}{I_n\cos\varphi_n}\Gamma_n.$$

For a traction motor, typical parameters values are so that: $I_{dn}/I_n \approx 5$ to 7 and $\cos\varphi_n \approx 0.8$ to 0.9. Thus: $I_{dn}/(I_n\cos\varphi_n) \approx 5.5$ to 9.

The maximal value of the reverse short circuit torque is then: $\Gamma_{\max} \cong 5.5$ to 9 Γ_n.

In the same way, if I_d is much larger than I_s, the (a) phase current maximum is obtained at $\Phi = \pi/2$ and is equal to:

$$i_{amax} = 2I_d\sqrt{2}. \tag{12}$$

This current value is reached half a period after the short circuit occurrence.

For the same typical parameters value, the maximal short circuit overcurrent value is: $i_{amax} \cong 14$ to 20 I_n.

4.1.4 Inclusion of damping effects

Another analytical formulations of three phase short circuit currents of an unloaded machine shows that they are damped with two time constants [1,15]: $T' = \sigma L_r/R_r$ which is the rotor time constant, stator in short circuit and $T_a = \sigma L_s/R_s$ which is the stator time constant, rotor in short circuit.

As stator and rotor currents include time constants T' and T_a, the electromagnetic torque which is given by (2) includes crossed components expressed by:

$$e^{-t/T'}\cdot e^{-t/T'}/e^{-t/T_a}\cdot e^{-t/T'}/e^{-t/T_a}\cdot e^{-t/T_a}.$$

Actually, leakage distribution factor of induction machines which power is high enough is so that σL_r can be assumed to be near σL_s. Moreover, R_s and R_r values are near in order to respect thermic balance conditions between stator and rotor parts.

Hence:

$$T' = \frac{\sigma L_r}{R_r} \approx \frac{\sigma L_s}{R_s} = T_a.$$

The crossed components can be therefore replaced by the central component

$$e^{-t\left(\frac{1}{T'}+\frac{1}{T_a}\right)}.$$

Then, an average time constant can be defined so that:

$$\frac{2}{\tau} = \left(\frac{1}{T'} + \frac{1}{T_a}\right) = \frac{R_s + R_r}{\sigma L_s}\,. \tag{13}$$

Hence, τ is approximately the damping time constant of phase currents and $\tau/2$ is the torque one. τ can be simply linked with the start-up power factor $\cos\varphi_d$. Indeed, start-up equations of the machine are so that:

$$\cos\varphi_d \cong \frac{R_s + R_r}{\sqrt{(\sigma L_s\omega_s)^2 + (R_s + R)^2}} \cong \frac{R_s + R_r}{\sigma L_s\omega_s}\,. \tag{14}$$

It can be deduced that:

$$\tau = \frac{2}{\omega_s\cos\varphi_d}\,. \tag{15}$$

As a result, damping effects are included in an average way and the expressions of damped phase currents and torque are given by:

$$i_a(t)\,(\text{with damping}) = i_a(t)\,(\text{without damping})\,e^{\frac{-t}{\tau}} \tag{16}$$

and:

$$\Gamma_{elm}(t)\,(\text{with damping}) = \Gamma_{elm}(t)\,(\text{without damping})\,e^{\frac{-2t}{\tau}}. \tag{17}$$

Hence, short circuit torque and current maximal values are given by:

$$\Gamma_{\max} = -\frac{I_{dn}}{I_n \cos\varphi_n} \Gamma_n e^{\left(-\frac{\pi}{2}\cos\varphi_d\right)} \tag{18}$$

$$i_{amax} = 2I_d\sqrt{2}e^{\left(-\frac{\pi}{2}\cos\varphi_d\right)}. \tag{19}$$

Damping factor is the same for overcurrent and reverse overtorque. Start-up operation of a traction motor is highly inductive which means that start-up current is limited by leakage inductances and : $\cos\varphi_d \approx 0.2$. The damping factor is thus equal to

$$e^{\left(-\frac{\pi\times 0.2}{2}\right)} \approx 0.2 \cong \frac{3}{4}$$

and the approximate values of current and torque maxima are given by: $\Gamma_{max} \cong 4$ to 7 Γ_n and $i_{amax} \cong 10$ to 15 I_n.

4.1.5 Inclusion of saturation effects

Expressions (9) and (10) take into account I_d value at short circuit initial conditions. This value is so high that it implies a saturated value of the motor leakage inductance.

Saturation of the leakage flux path is then included in the analytical formulation by a constant parameter which is I_d.

On the other hand, non saturation of the main flux path is not taken into account since expressions (9) and (10) are function of the initial steady-state current I_s which value is given, at near nominal conditions, for saturated magnetizing inductance.

However, it should be noted that this approximation has not a lot of influence on the analytical formulation accuracy because the dominant components of (9) and (10) are depending mainly on I_d.

4.1.6 Inclusion of deep-bar effects

Following (15), (16) and (17), three phase short circuit torque and currents are function of the value of $\cos\varphi_d$ at the supply frequency. Therefore, the results given by the analytical formulation includes, approximately, current displacement effects on rotor resistance and leakage inductance during the short circuit.

4.2 Presentation of the results

4.2.1 Analytical results

The results given by single cage analytical formulation are compared with those presented for the finite element modeling. Values of the formulation parameters are obtained from finite element computations of no-load and blocked rotor tests [8,16]. They are summed up in Table 1. In accordance with finite element and analytical investigations, they correspond to:

Table 1. Single cage model parameters values.

Parameter	Value
R_s at 20 °C(mΩ)	22
R_r at 20 °C(mΩ)	18.6
L_s (mH)	18.6
σL_s (mH)	1.3

Table 2. Initial condition values.

Variable	Values
V_s (V)	1200
I_s (A)	583
ω_s (rad/s)	$2\pi \times 51$
$\cos\varphi$	0.85

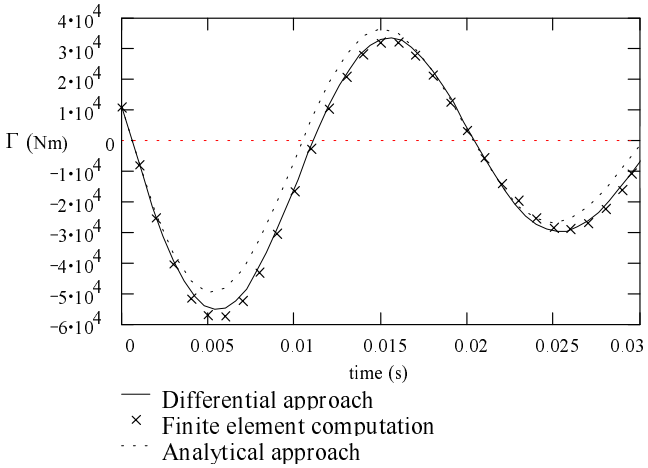

Fig. 10. Three phase short circuit torque.

- Constant leakage inductances values calculated at the assumed short circuit current value (about 10 to 15 I_n);
- Constant magnetizing inductance value obtained for the initial conditions preceding the short circuit occurrence;
- Constant resistances values taking into account skin effect at the initial supply frequency of the motor.

The initial operating point in accordance with these parameters and the finite element computation is presented in Table 2. A comparison between short circuit torque waveforms is shown in Figure 10. The difference on the maximal value of the torque is near 15%.

4.2.2 Differential approach results

In order to improve results accuracy, the differential system (1) is numerically integrated without assumptions on the resistance values.

As illustrated in Figure 10, the remaining difference between the finite element computation and the differential approach is low, about 5% for the torque peak.

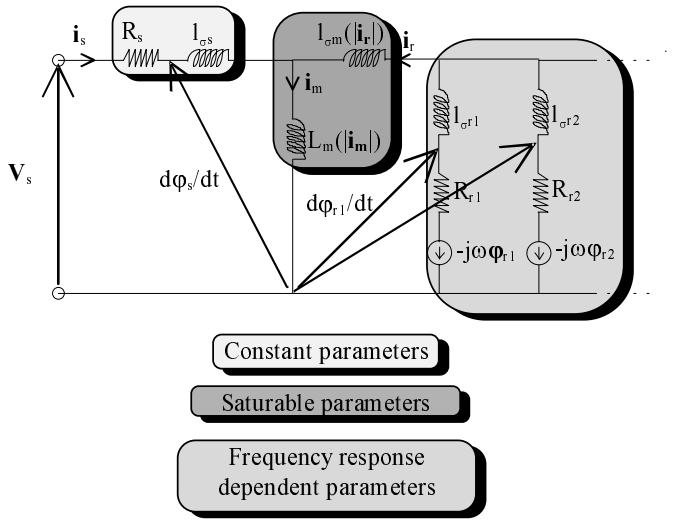

Fig. 11. Improved equivalent circuit of a cage induction machine.

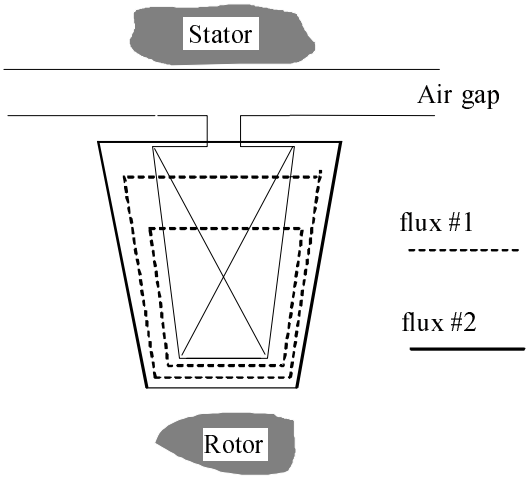

Fig. 12. Rotor bar leakage flux paths.

5 Use of improved equivalent circuits

In order to generalize the differential approach, which application is much easier than the finite element one, an improved equivalent circuit of the traction motor can be identified [16]. This circuit, as presented in Figure 11, derives from the saturated equivalent circuit shown in Figure 3.

The main features of this model are introduced in [16] and can be summed up by the following points:

- L_m is assumed to be independent of the frequency because of cores lamination;
- the number of parallel rotor branches is increased so that the equivalent circuit is able to represent with accuracy and constant parameters the motor frequency response over a large frequency scale;
- Saturation effects are included by saturable inductances.

Hence, if deep-bar effect is required to be modeled by constant parameters, rotor leakage inductance has to be divided into a saturated part and a frequency dependent one. A justification of this partition can be given by considering the leakage flux sources in a cage rotor. The rotor leakage inductance includes slot leakage inductances, differential inductances and end ring leakage inductance. Differential and end ring flux flow mainly through the air. Corresponding inductances can therefore be assumed to be only frequency dependent.

On the other hand, the slot leakage inductance can be divided into two parts as shown in
Figure 12. One is related to the leakage flux crossing through the rotor slot (flux #1), and the other corresponds to the flux #2 across the slot bridge. The first part depends mainly on the distribution of current density in the slot whereas the second part is produced by the total mmf and flows almost entirely along the teeth. Hence, the first part of the rotor slot leakage inductance is assumed to be only frequency dependent and the second part is supposed to be influenced only by the total rotor slot current.

Finally, rotor leakage inductance is divided into a saturable inductance l_{σ^m} and a frequency dependent part which includes differential, end ring inductances and the leakage inductance related to flux #1. This frequency dependent inductance is represented in the equivalent circuit by the parallel rotor branches.

All the parameters values and variations are obtained by finite element computations. It should be noted that the validity of the separation of deep bar and saturation effects can be verified for the studied traction motor. The parameters values are given in Table 3 for the 1.5 MW - 4 poles traction motor.

The improved equivalent circuit is used to compute three phase short circuits. The resulting short circuit torque is compared in Figure 13 with the torque given by the finite element simulation. There is almost no difference in amplitude and phase.

Table 3. Improved equivalent circuit parameters values.

Parameter	Value
R_s (m Ω)	22.04
$l_{\sigma s}$ (mH)	0.89
L_m	fonction of I_m
$l_{\sigma m}$ (mH)	fonction of I_r
R_{r1} (m Ω)	15.04
$l_{\sigma r1}$ (mH)	0.67
R_{r2} (m Ω)	1.65
$l_{\sigma r2}$ (mH)	3.93
R_{r3} (Ω)	18.51
$l_{\sigma r3}$ (mH)	5.59

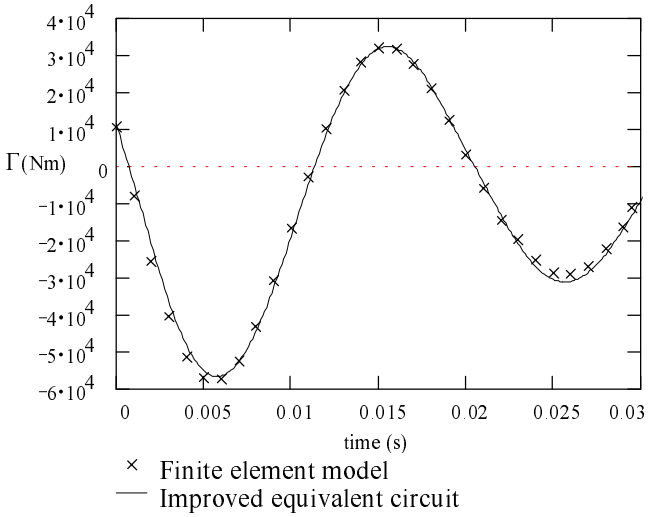

Fig. 13. Three phase short circuit torque.

6 Conclusion

In this paper, three ways of studying three phase short circuits of traction motors have been presented. Each of one is more or less easy to apply and provides more or less complete and accurate results.

A single cage equivalent circuit is an accurate model of the studied traction motor during three phase short circuit operations if saturation effects are modeled. Indeed, the rotor cage dimensions are so that the use of higher order equivalent circuit is not justified to take into account skin effect in the rotor bars. However, the identification of an improved equivalent circuit is possible based on the finite element modeling of the motor. This circuit has been tested for three phase short circuit simulations but can also be included in a global model of an induction motor drive used to investigate fault modes in simulation [25]. The finite element modeling provides the more extensive results but the computation requires several days on a UNIX workstation HP model 712/20 – 64 Mo whereas the improved equivalent circuit only requires a few minutes on a Pentium PC 75 MHz–32 Mo.

The complete validation of the three methods requires experimental tests of three phase short circuits. These tests have been performed for a 30 kW - 4 pole double cage induction machine. They have been used to validate the analytical formulation and the improved equivalent circuit under unsaturated conditions [29]. In conclusion, the whole results obtained for the traction and industrial motors reasonably indicate that the improved model is valid even under saturated conditions.

The authors gratefully thank P. Mannevy (SNCF - French Railway Company) and M. Roger (GEC Alsthom Ornans) for their support and participation to this study.

References

1. P. Vas, *Electrical Machines and Drives - A Space Vector Theory Approach* (Clarendon Press, Oxford, 1992).
2. P.L. Alger, *Induction Machines* (Gordon and Breach Science Publishers, New-York, Second Edition, 1970).
3. P.L. Alger, M. Ivanès, M. Poloujadoff, Electric Machines Electromech. **2**, 137 (1978).
4. T.A. Lipo, A. Consoli, IEEE Trans. Industry Appl. **IA-20**, 180 (1984).
5. I. Boldea, S.A. Nasar, IEE Proc B **134**, 355 (1987).
6. G.R. Slemon, in *IEEE/IAS Annual Meeting conference record*(1998) p 111.
7. A. Keyhani, H. Tsai, IEEE Trans. Energy Conv. **4**, 1, 118 (1989).
8. A. Taieb Brahimi, Ph.D. thesis INPG, Grenoble, 1994.
9. M.M. Liwschitz, Garik, AIEE Trans. on Power Apparatus and System III **74**, 768 (1955).
10. R.C. Healey, S. Williamson, A.C. Smith, IEEE Trans. on Industry Appl. **31**, 4, 812 (1995).
11. D. Zhu, Ph.D. thesis INPG, Grenoble, 1990.
12. R. Palma, S.J. Salon, M.J. DeBortoli, in *Proceedings of the International Conference on Electric Machines*, (Cambridge, USA, 1990).
13. H.A. Toliyat, T.A. Lipo, IEEE Trans. on Energy Conversion **10**, 2, 241 (1995).
14. X. Luo, Y. Liao, H. Toliyat, A. El-Antably, T. Lipo, in *IEEE/IAS Annual Meeting conference Record* (1993) p. 203.
15. P. Barret, Régimes transitoires des machines électriques tournantes (Eyrolles, Paris, 1986).
16. N. Retière, A. Foggia, D. Roye, P. Mannevy, in *IEEE International Electric Machines and Drives Conference Record*, Milwaukee (USA), 18-21 Mai (1997).
17. P.C. Krause, *Analysis of Elecric Machinery* (McGraw-Hill Book Company, New-York, 1986).
18. Salon, D.W. Burow, R.E. Ashley III, L. Ovacik, M.J. De Bortoli, IEEE Trans. Magn. **MAG-29**, 1438 (1993).
19. S.I. Moon, A. Keyhani, in *IEEE/IAS Annual Meeting conference record* (1993), p. 336.
20. P. Lombard P. and G. Meunier, IEEE Trans. Magn. **MAG-28**, 1291 (1992).
21. E. Vassent, G. Meunier, A. Foggia and J.C. Sabonnadiere, in *IMACS-TC1 Conference*, Nancy, France, **1** (1990) p. 221.
22. S.S. Kalsi, IEEE Trans. on PAS, **PAS-92**, 1266 (1974).
23. O. Sahraoui, Ph.D. thesis INPG, Grenoble, 1994.
24. E. Vassent, G. Meunier, A. Foggia, in *4th Biennial IEEE Conference on Electromagnetic Field Computation*, Toronto Canada, (1990).
25. N. Retière, L. Gerbaud, P.J. Chrzan, D. Roye, P. Mannevy, in *7th European Conference on Power Electronics and Applications* Trondheim (1997).
26. N. Retière, D. Roye, P. Mannevy,in *IEEE/PESC'97 Conference Proc.* St Louis, (1997).
27. R. Peuget, S. Courtine, J.P. Rognon, in *IEEE/IAS'97 Conference Proc.*, New Orleans, (1997).
28. P.J. Chrzan, R. Szczesny,in *IEEE/ISIE'96 Conference Proc.*, Warsaw, **2**, 1011 (1996).
29. N. Retière, P.J. Chrzan, M. Ivanès, D. Diallo, Electric Machines Power Syst. **27**(4),(1998).